Short title: PREDICTION ERROR IN MOTOR ADAPTATION

# Distinct Neural Signatures of Reward and Sensory Prediction Error in Motor Learning

Dimitrios J. Palidis[1,2,3], Joshua G. A. Cashaback[1,2], Paul L. Gribble[1,2,4,5,*]

[1]The Brain and Mind Institute, The University of Western Ontario, London, ON, Canada

[2]Dept. Psychology, The University of Western Ontario, London, ON, Canada

[3]Graduate Program in Neuroscience, The University of Western Ontario, London, ON, Canada

[4]Dept. Physiology & Pharmacology, Schulich School of Medicine & Dentistry, The University of Western Ontario, London, ON, Canada

[5]Haskins Laboratories, New Haven, CT, USA

* Corresponding author

Email: paul@gribblelab.org

Acknowledgements: We thank Heather McGregor for help with the EEG recordings

**Abstract**

Two distinct processes contribute to changes in motor commands during reach adaptation: reward based learning and sensory error based learning. In sensory error based learning, the mapping between sensory targets and motor commands is recalibrated according to error feedback. In reward based learning, motor commands are associated with subjective value, such that successful actions are reinforced. We recorded EEG from humans of either sex to identify and dissociate the neural correlates of reward prediction error (RPE) and sensory prediction error (SPE) during learning tasks designed to isolate each response. We designed a visuomotor rotation task to isolate sensory error based learning in response to SPE, which was induced by altered visuospatial feedback of hand position. In a reward learning task, we isolated learning in response to RPE, which was induced by binary reward feedback. We found that a fronto-central event related potential called the feedback related negativity occurred specifically in response to RPE during reward based learning, while a more posterior component called the P300 was associated with SPE during a visuomotor rotation task. These findings reveal a dissociation between well characterized EEG signatures of error processing in two distinct motor learning processes.

**Significance Statement**

Adaptation of motor output to changing task demands and dynamic environments is thought to occur on the basis of distinct forms of prediction error. Reward prediction error occurs when the subjective value of an outcome is different than the expected value, while sensory prediction error occurs when the low-level sensory consequences of motor commands are different than predicted. It remains unclear how EEG activity patterns associated with error processing apply to these distinct forms of motor adaptation. We found that an event related potential component called the feedback related negativity responded only to reward prediction error, while the P300 component is modulated by sensory prediction error and correlated to sensory error based learning.

## Introduction

It is thought that sensorimotor adaptation is driven by two distinct error signals, sensory prediction error (SPE) and reward prediction error (RPE), and that both can simultaneously contribute to learning (Huang et al., 2011; Izawa and Shadmehr, 2011; Shmuelof et al., 2012; Galea et al., 2015; Nikooyan and Ahmed, 2015). EEG has been used to identify neural signatures of error processing in various motor learning and movement execution tasks, but it remains unclear how these neural responses relate to distinct reward and sensory-error based motor learning mechanisms (Krigolson et al., 10/2008; Torrecillos et al., 2014; MacLean et al., 2015). Here we identified distinct neural signatures of SPE and RPE in motor learning using separate learning paradigms that produce comparable changes in behavior.

SPE occurs when the visuospatial consequences of motor commands differ from the expected outcomes. SPEs can be imposed in experimental visuomotor rotation (VMR) paradigms by rotating visual feedback of hand position relative to the actual angle of reach. Adaptation, in which motor output is adjusted to compensate for perturbations, is thought to be driven primarily by SPE in these tasks (Izawa and Shadmehr, 2011; Marko et al., 2012). Sensory error feedback activates brain regions including primary sensory motor areas, posterior parietal cortex, and cerebellum (Inoue et al., 2000; Krakauer et al., 2004; Diedrichsen et al., 2005; Bédard and Sanes, 2014). Tanaka et al., (2009) propose that SPEs computed by the cerebellum produce adaptation via changes in synaptic weighting between the posterior parietal cortex and motor cortex.

Recent research suggests that a reward based learning process can also contribute to motor adaptation in parallel to a sensory-error based learning system, and that reward

feedback can drive motor learning even in the absence of sensory error feedback (Izawa and Shadmehr, 2011). Reward learning has been isolated experimentally by providing participants only binary reward feedback, without visual feedback of hand position. Reward-based motor learning has been modelled as reinforcement learning, which maps actions to abstract representations of reward or success, rather than to low level sensory consequences of action. In reinforcement learning, if the outcome of an action is better than its expected value, a positive RPE occurs which drives an increase in the expected value and future likelihood of selecting that particular action. Conversely, if the outcome is worse than expected, a negative RPE diminishes the expected value and likelihood of selecting that action. Phasic dopaminergic signaling in the VTA and striatum is consistent with encoding of a RPE (Glimcher, 2011), and dopaminergic activity has been implicated in reward based motor learning (Galea et al., 2013; Se et al., 2015).

EEG has been used to identify neural correlates of error monitoring, but few studies have employed motor adaptation tasks. An event-related potential (ERP) known as the feedback related negativity (FRN) has been proposed to reflect processing of RPE in the context of reinforcement learning. There is evidence that FRN reflects the activity in anterior cingulate or supplementary motor cortical areas, and it is theorized to be driven by phasic dopaminergic signaling of RPE (Walsh and Anderson, 2012). The FRN potential is superimposed on the P300, a well characterized positive ERP component that peaks later than FRN, and with a more posterior scalp distribution. It has been proposed that the P300 reflects the updating of a model of stimulus context (Donchin and Coles, 1988). Both components have been observed in response to errors in motor tasks. In this paper we describe experiments in which we isolate

and compare EEG responses to both RPE and SPE using separate adaptation paradigms that produce comparable changes in behavior. We test the idea that the FRN is a neural signature of reward based motor learning behavior while the P300 reflects sensory error based learning.

## Material and Methods

**Experimental Design and Statistical Analysis.** Participants underwent alternating experimental blocks of a reward learning task and a visuomotor rotation task. The design for each task is described under “reward learning task” and “visuomotor rotation task” methods subsections, respectively. Results of statistical tests are reported in the Results section, under “Behavioral Results”, “Feedback Related Negativity Results”, and “P300 Results”. T-tests and Pearson’s linear correlation tests were performed using MATLAB R2016b, and ANOVAs were conducted using IBM SPSS Statistics version 25.

***Participants*.** A total of $n$ = 13 healthy, right-handed participants were included in our study (24.68 ± 2.74 years old, 10 females). Three participants underwent the experimental procedure but were excluded due to malfunction of the EEG recording equipment. One participant who reported that they performed movements based on a complex strategy that was unrelated to the experimental task, was excluded. Participants provided written informed consent to experimental procedures approved by the Research Ethics Board at The University of Western Ontario.

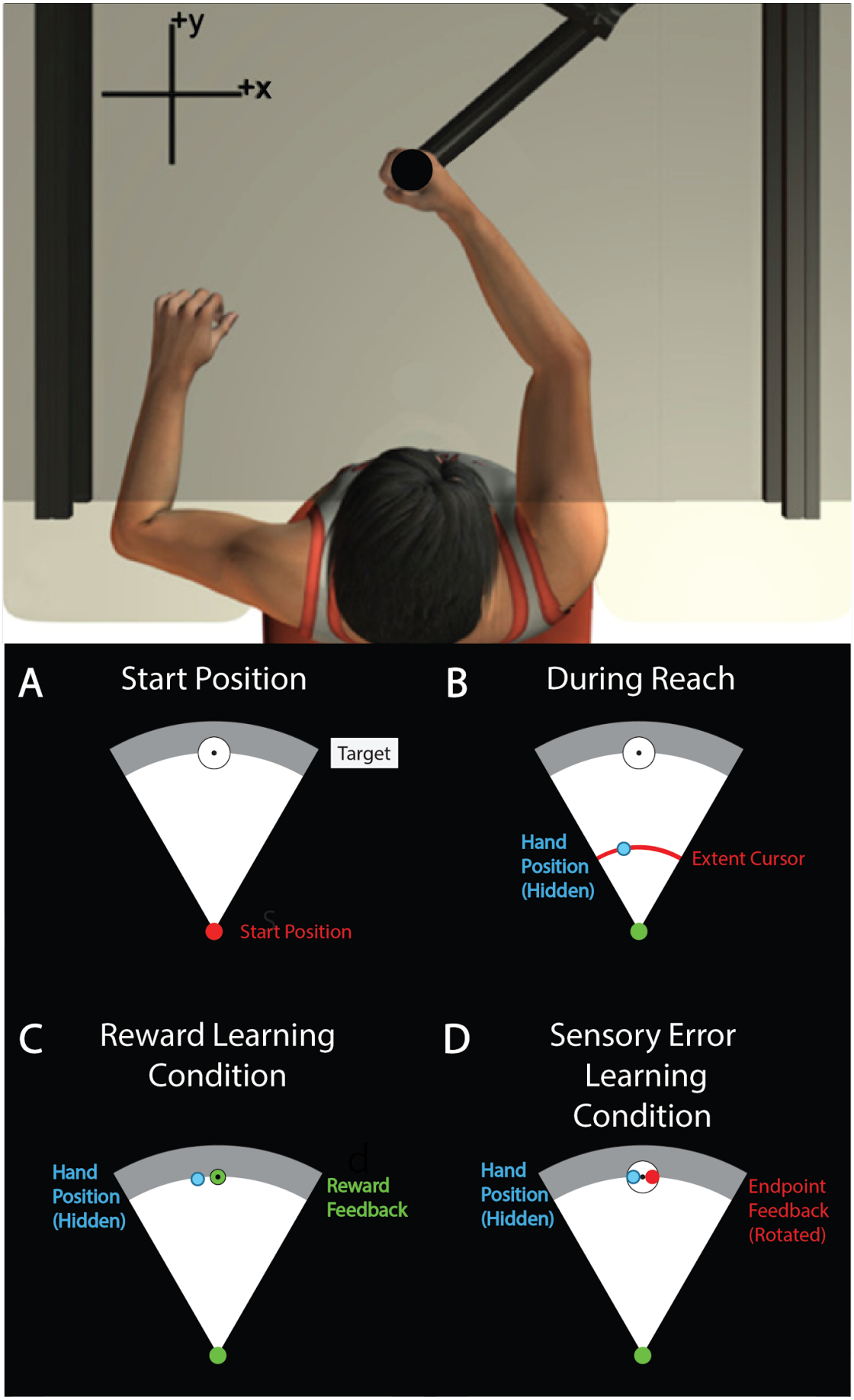
+y
+x
A
Start Position
Target
Start Position
B
During Reach
Hand Position (Hidden)
Extent Cursor
C
Reward Learning Condition
Hand Position (Hidden)
Reward Feedback
D
Sensory Error Learning Condition
Hand Position (Hidden)
Endpoint Feedback (Rotated)

124 ***Figure 1.*** *Experimental setup.* ***A****, Participants reached to visual targets while holding the handle of a robotic arm.*
125 *Vision of the arm was obscured by a screen that displayed visual information related to the task.* ***B,*** *During reaches,*
126 *hand position was hidden but an arc shaped cursor indicated the extent of the reach without revealing reach angle.*
127 *Feedback was provided at reach endpoint.* ***C,*** *In the reward learning condition, binary feedback represented*
128 *whether reaches were successful or unsuccessful in hitting the target by turning green or red, respectively. Reach*
129 *adaptation was induced by providing reward for movements that did not necessarily correspond to the visual*
130 *target.* ***D,*** *In the visuomotor rotation condition, feedback represented the endpoint position of the hand. Adaptation*
131 *was induced by rotating the angle of the feedback relative to the actual reach angle.*
132
133 ***Experimental Procedure.*** Participants first performed a block of 50 practice trials. After the
134 practice block the experimenter fitted the EEG cap and applied conductive gel to the electrodes
135 before beginning the behavioral task (see "EEG Data Acquisition" below). The behavioral task
136 consisted of 8 experimental blocks, including four 115-trial blocks of a reward learning task and
137 four 125-trial blocks of a visuomotor rotation task. The order of the blocks alternated between
138 the two task types but was otherwise randomized. Participants took self-paced rests between
139 blocks.
140
141 ***Apparatus/Behavioral Task****.* Participants produced right-arm reaching movements in a
142 horizontal plane at chest height while holding the handle of a robotic arm (InMotion2,
143 Interactive Motion Technologies, Massachusetts, United States; Fig 1). Position of the robot
144 handle was sampled at 600 Hz. A semi-silvered mirror obscured vision of the arm and displayed
145 visual information related to the task. An air-sled supported each participant's right arm.

Participants began each trial with their hand at a start position in front of their chest at body midline (mid-saggital plane). The start position was a circle with a diameter of 1 cm, and was rendered as a red circle on the visual display (Fig 1a). A white circular target was displayed 14 cm away from the start position (Fig 1a). A cursor indicated hand position within the start position. The start position turned green to cue the onset of each reach once the handle had been inside the start position continuously for 750 ms. Participants were instructed that they must wait for the cue to begin each reach, but that it was not necessary to reach immediately or react quickly upon seeing the cue.

Participants were instructed to make forward reaches and to stop their hand within the target. An arc shaped cursor continuously indicated the reach extent, without revealing the angle of the hand relative to the start position. Continuous position feedback was provided in the first 5 baseline trials of each block, and consisted of an additional circular cursor indicated the position of the hand throughout the reach. In all subsequent reaches for each block, the cursor indicating hand position disappeared when the hand left the start position, and only the arc shaped cursor indicating movement extent was shown. A viscous force field assisted participants in braking their hand when the reach extent was greater than 14 cm.

The robot ended each movement by fixing the handle position when the hand velocity decreased below 0.03 m/s. During this time, while the hand was fixed in place (for 700 ms) visual feedback of hand position was provided. Feedback indicated either reach endpoint position, a binary reward outcome, or feedback of movement speed (see below). Visual feedback was then removed and the robot guided the hand back to the start position. During this time no visual information relating to hand position was displayed.

Reach endpoint was defined as the position at which the reach path intersected the perimeter of a circle (14 cm radius), centered at the start position. Reach angle was calculated as the angle between a line drawn from the start position to reach endpoint and a line drawn from the start position to the center of the target, such that reaching straight ahead corresponds to 0 degrees and counter-clockwise reach angles are positive (Fig 1a). Feedback about reach angle was provided either in the form of endpoint position feedback or binary reward feedback. The type of feedback, as well as various feedback manipulations, varied according to the assigned experimental block type (See “Reward Learning Condition” and “Visuomotor Rotation Condition”). Endpoint position feedback consisted of a static cursor indicating the position of movement endpoint, while reward feedback consisted of the target turning either red or green to indicate that the reach endpoint missed or hit the target, respectively.

Movement duration was defined as the time elapsed between the hand leaving the start position and the moment hand velocity became less than 0.03 m/s. If movement duration was greater than 700 ms or less than 450 ms no feedback pertaining to movement angle was provided. Instead, the gray arc behind the target turned blue or yellow to indicate that the reach was too slow or too fast, respectively. Participants were informed that movements with an incorrect speed would be repeated but would not otherwise affect the experiment.

To minimize the impact of eye-blink related EEG artifacts, participants were asked to fixate their gaze on a black circular target in the center of the reach target and to refrain from blinking throughout each arm movement and subsequent presentation of feedback.

***Practice Block.*** Each participant completed a block of practice trials before undergoing the reward learning and visuomotor rotation experiments. Practice continued until participants achieved 50 movements within the desired range of movement duration. Continuous position feedback was provided during the first five trials, and only endpoint position feedback was provided for the subsequent 10 trials. After these initial 15 trials, no position feedback was provided outside the start position.

***Reward Learning Task*.** Binary reward feedback was provided to induce adaptation of reach angle. Each participant completed 4 blocks in the reward learning condition. We manipulated feedback with direction of intended learning and reward probability as factors using a 2x2 design (direction of learning x reward probability) across blocks. For each direction of intended learning (clockwise and counter-clockwise), each participant experienced a block with high reward probability and a block with low reward probability. Each reward learning block continued until the participant completed 115 reaches with acceptable movement duration. Participants reached towards a circular target 1.2 cm (4.9 deg) in diameter. The first 15 reaches were baseline trials during which the participant did not receive reward feedback. Continuous position feedback was provided during the first five trials, and only endpoint position feedback was provided for the subsequent 10 trials. After these baseline trials, no position feedback was provided, and binary reward feedback was provided at the end of the movement. Participants were told that they would earn some additional monetary compensation for reaches that ended within the target, up to a maximum of $10 for the whole experiment. Participants were

told that rewarded and unrewarded reaches would be indicated by the target turning green and red, respectively.

Unbeknownst to participants, reward feedback was delivered probabilistically. The likelihood of reward depended on the difference between the current reach angle and the median reach angle of the previous 10 reaches. In the high reward probability condition, reward was delivered with probability of 100% if the difference between the current reach angle and the running median was in the direction of intended learning, and at a probability of 30% otherwise (Eq. 1). When the running median was at least 6 degrees away from zero in the direction of intended learning, reward was delivered at a fixed probability of 65%. This was intended to minimize conscious awareness of the manipulation by limiting adaptation to +-6 degrees. In the low reward probability condition, reward was similarly delivered at a probability of either 70% or 0% (Eq. 2). When the running median was at least 6 degrees away from zero in the direction of intended learning, reward was delivered at a fixed probability of 35%. Reach angle and feedback throughout a representative experimental block is shown in figure 2.

Eq. 1:

$$p_{high} = \begin{cases} 1 \quad , & z \cdot (\theta_i - median(\theta_{i-10}, \dots, \theta_{i-1})) > 0 \\ .30 \quad , & z \cdot \left(\theta_i - median(\theta_{i-10}, \dots, \theta_{i-1})\right) < 0 \\ .65 \quad , & z \cdot median(\theta_{i-9}, \dots, \theta_i) > 6 \end{cases}$$

Eq. 2:

$$p_{low} = \begin{cases} .70 & , \quad z \cdot (\theta_i - median(\theta_{i-10}, \dots, \theta_{i-1})) > 0 \\ 0 & , \quad z \cdot (\theta_i - median(\theta_{i-10}, \dots, \theta_{i-1})) < 0 \\ .35 & , \quad z \cdot median(\theta_{i-9}, \dots, \theta_i) > 6 \end{cases}$$

Where $p$ is probability of reward described separately for the high and low reward probability conditions, $\theta_i$ is the reach angle on trial *i,* z=1 for counter-clockwise learning blocks, and z = -1 for clockwise learning blocks.

***Visuomotor Rotation Task.*** Endpoint feedback was rotated relative to the actual reach angle to induce sensory-error based adaptation. Each participant completed 4 blocks in the visuomotor rotation condition. We manipulated feedback with initial rotation direction and perturbation size as factors using a 2x2 design across blocks. For each direction of initial rotation (clockwise and counter-clockwise) each participant experienced a block with large rotation (1.5 deg) and a block with small rotation (.75 deg). Each block continued until participants completed 125 reaches within acceptable movement duration limits. Participants reached towards a circular target 2.5 cm (10.2 deg) in diameter. Participants first performed 25 baseline reaches during which position feedback reflected veridical reach angle. A cursor continuously indicated hand position during the first 10 trials. A static cursor indicated movement endpoint position for the subsequent 15 trials. After the baseline reaches, the adaptation portion of each block began

unannounced to participants and continued until the participant performed 100 additional reaches of acceptable movement duration.

During the adaptation trials, endpoint position feedback was provided that did not necessarily correspond to the true hand position. Participants were instructed that endpoint feedback within the target would earn them bonus compensation, but no explicit reward feedback was provided. In a randomly selected 50% of trials, a rotation of 0.75 deg or 1.5 degs was imposed in the small and large perturbation conditions, respectively. In addition to adding a fixed rotation to the feedback angle in 50% of trials, we subtracted an estimate of the current state of reach adaptation from the feedback angle for every trial (Eq. 3). This accounted for behavioral adaptation, allowing us to keep the average visual error size in the unperturbed and perturbed trials approximately constant throughout the experiment, despite participants adapting their reach angle to counteract the perturbations.

The online estimate of adaptation consisted of a running average of the previous 6 reach angles and a model of reach adaptation which assumed that participants would adapt to a fixed proportion of the reach errors experienced during the previous 3 trials. A windowed average centered around the current reach angle could serve as a low pass filter to estimate the current state of reach adaptation, but the running average during the experiment was necessarily centered behind the current reach angle. Thus, an online model was necessary to account for adaptation that would occur in response to errors experienced on trials included in the running average. Misestimation of the learning rate in the online model would lead to systematic bias in the feedback angle, while a perfect model would lead to unperturbed feedback that is distributed around 0 deg with variance that reflects the natural movement

variability. Thus, an adaptation rate of 0.25 was chosen for the online model on the basis of pilot data, as we found that it resulted in a mean visual error of approximately zero in non-rotated trials.

As in the reward learning condition, we sought to limit the magnitude of adaptation to 6 degrees in an attempt to minimize conscious awareness of the manipulation. This limit was implemented by reversing the direction of the perturbation whenever the average reach angle in the previous 6 movements differed from 0 by at least 6 deg in the direction of intended reach adaptation. Reversing the direction of the perturbation caused participants to begin adapting in the opposite direction. Reach angle and feedback angle throughout a representative experimental block is shown in figure 2.

Eq.3:

$$\boldsymbol{X_i} = \theta_i + q - mean(\theta_{i-6}, \dots, \theta_{i-1}) + \sum_{k=i-3}^{i-1} (.25 \cdot x_k)$$

$$q = z \cdot s \cdot u$$

$$p(u = 0) = 0.5$$
$$p(u = 1) = 0.5$$

Where $X$ denotes feedback angle, θ denotes reach angle, and $q$ denotes perturbation. $z$ denotes the direction of the perturbation (z=1 for counter-clockwise perturbations, and z = -1 for clockwise perturbations). $S$ denotes the size of the perturbation (.75 or 1.5 in the small and

large error conditions, respectively). $\mathcal{U}$ is a discrete random variable that is realized as either 1 or 0 with equal probability (50%).

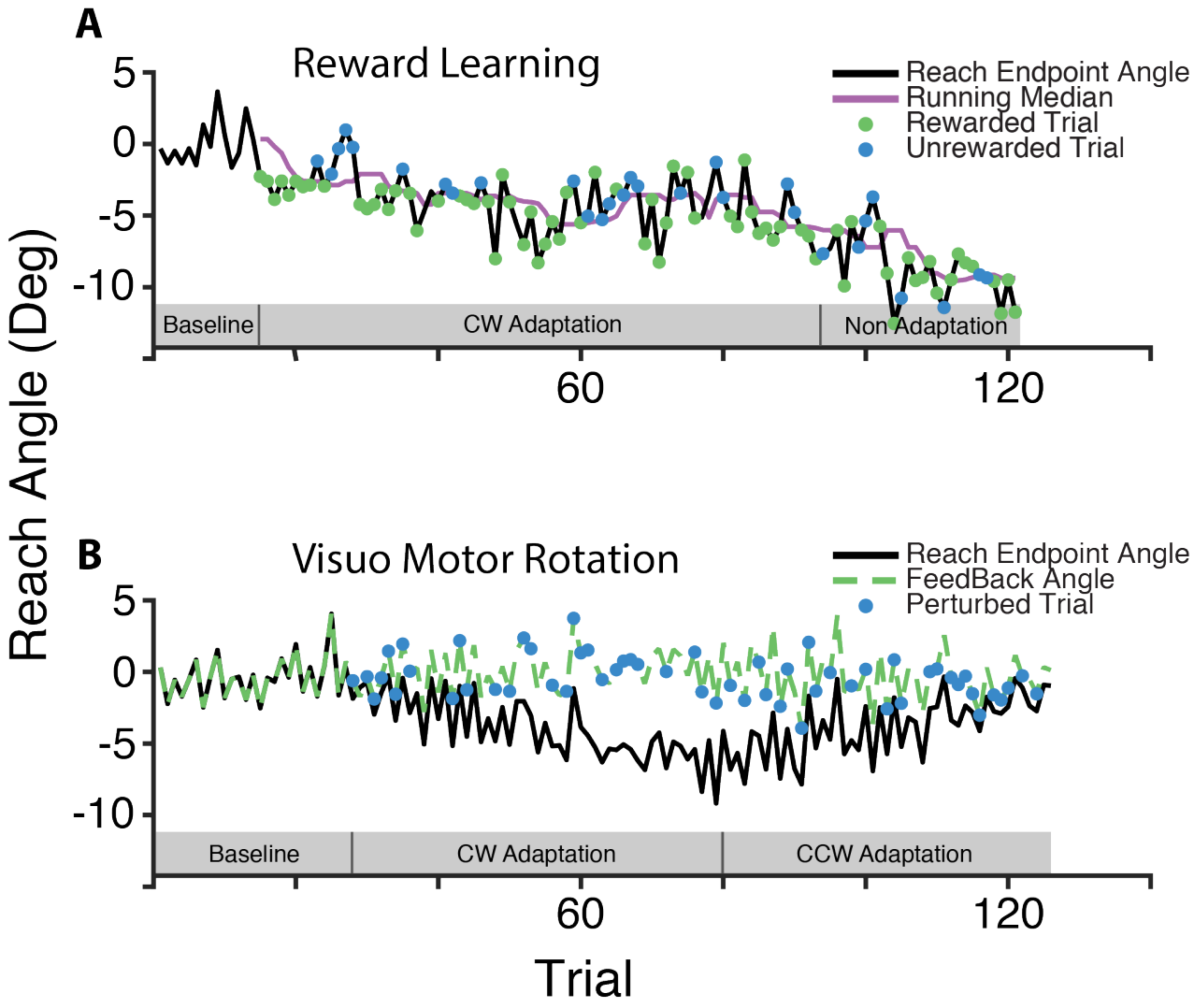


***Figure 2.*** *Reach angles of a representative participant.* ***A,*** *We show the reward learning block assigned to the clockwise adaptation with high reward probability condition. Reaches were rewarded with 100.0% probability for reach angles less than the median of the previous 10 reaches, and with 30.0% probability for reach angles greater than this running median. Reward was delivered at a fixed probability of 65.0% when the running median was less than -6 degrees.* ***B,*** *The visuomotor rotation block assigned to the 1.5 degree rotation condition is shown. The*

*rotation is imposed randomly in 50% of trials. The rotation is initially counterclockwise but reverses when the mean of the previous five reach angles becomes less than -6.0 degrees.*

**EEG Data Acquisition.** EEG data were acquired from 16 cap-mounted electrodes using an active electrode system (g.Gamma; g.tec Medical Engineering) and amplifier (g.USBamp; g.tec Medical Engineering). We recorded from electrodes placed according to the 10-20 system at sites Fz, FCz, Cz, CPz, Pz, POz, FP1, FP2, FT9, FT10, FC1, FC2, F3, F4, F7, F8, referenced to an electrode placed on participants' left earlobe. Impedances were maintained below 5 kU. Data were sampled at 4,800 Hz and filtered online with band-pass (0.1–1,000 Hz) and notch (60 Hz) filters. The amplifier also recorded data from a photo-diode attached to the display monitor to determine the timing of stimulus onset.

**Behavioral Data Analysis.** *Reward learning task:* Motor learning scores were calculated for each participant as the difference between the average reach angle in the counter-clockwise learning blocks and the average reach angle in the clockwise learning blocks. We excluded baseline trials and trials that did not meet the movement duration criteria.

*Visuomotor rotation task:* To quantify trial-by-trial learning we first calculated the change in reach angle between successive trials, $\Delta\theta_i$, as in Equation 4:

Eq. 4: $$\Delta\theta_i = \theta_{i+1} - \theta_i$$

We then performed a linear regression on $\Delta\theta_i$ with the rotation imposed on the preceding trial as the predictor variable. The rotation was either 0, ±0.75, or ±1.5 deg. This regression was performed on an individual participant basis, using the data from the adaptation portion of all four visuomotor rotation blocks. We excluded trials that did not meet the duration criteria or that resulted in a visual error of > 10 degrees (mean= 0.79 trials per participant, SD= 1.24), as these large errors were thought to reflect execution errors or otherwise atypical movements. We took the unsigned value of the resulting slope estimate as a metric of learning rate for each participant, as it reflects the portion of visual errors that participants corrected with a trial-by-trial adaptive process.

**EEG Data Denoising.** EEG data were band-pass filtered offline between 0.5-35 Hz using a second order Butterworth filter. Continuous data were segmented into 2 second epochs time-locked to feedback stimulus onset at 0 ms (time range: -500 to +1500 ms). Epochs containing artifacts were removed using a semi-automatic algorithm for artifact rejection in the EEGLAB toolbox (see Delorme and Makeig, 2004 for details). Epochs flagged for containing artifacts as well as any channels with bad recordings were removed after visual inspection. Subsequently, extended infomax independent component analysis was performed on each participant's data (Delorme and Makeig, 2004). Components reflecting eye movements and blink artifacts were identified by visual inspection and subtracted by projection of the remaining components back to the voltage time series.

**Event Related Component Averaging.** We computed event related potentials (ERPs) on an individual participant basis by trial averaging EEG time series epochs after artifact removal. We selected trials corresponding to various feedback conditions in each task as described below. For each feedback condition ERPs were computed on an individual participant basis separately for recordings from channels fcZ and pZ. All ERPs were baseline corrected by subtracting the average voltage in the 100 ms period preceding stimulus onset. Trials in which reaches did not meet the movement duration criteria were excluded.

*Reward Learning Task:* ERPs from the reward learning condition were used to examine the neural correlates of RPE. We computed ERPs separately for feedback conditions corresponding to “expected reward”, “unexpected reward”, “expected non-reward”, and “unexpected non-reward”. Expectancy was determined on the basis of the reward probability condition: reward in the high reward probability and non-reward in the low reward probability conditions were deemed expected, while reward in the low reward probability and non-reward in the high reward probability conditions were deemed unexpected (Holroyd and Krigolson, 2007).

*Visuomotor Rotation Task:* ERPs elicited by visuomotor rotation were used to examine the neural correlates of SPE. First, we computed ERPs to compare the neural responses for rotated and non-rotated endpoint position feedback. This comparison occurs within blocks as rotations were imposed in a randomly selected 50% of trials. We created trial averaged ERP responses for trials with rotated feedback and trials with non-rotated feedback separately for the 0.75 deg

362 and 1.5 deg rotation conditions. The resulting ERPs are identified by the conditions “rotated
363 0.75 deg”, “non-rotated 0.75 deg”, “rotated 1.5 degs” and “non-rotated 1.5 deg”.

364 For the non-rotated trials we used an estimate of the current state of adaptation to
365 deliver feedback to the predicted endpoint position of the hand. The more unreliable this
366 estimate was, the more SPE would have occurred in the non-rotated trials. Furthermore, it has
367 been shown that when using an explicit aiming strategy to successfully compensate for a VMR,
368 the discrepancy between the hand position and feedback still produces a SPE that drives an
369 implicit form of adaptation (Mazzoni and Krakauer, 2006). Depending on how much the
370 adaptation in our task was achieved through strategic aiming, the non-rotated trials could still
371 induce SPE even if our estimate of the state of adaptation was completely reliable.

372 Because the non-rotated trials could still induce SPE, we also computed ERPs to
373 compare the neural response between blocked feedback conditions irrespective of the
374 randomly imposed rotations. We computed “small error” and “large error” ERPs including all
375 trials of the adaptation portion of the visuomotor rotation blocks for the 0.75 degrees and 1.5
376 degrees rotation conditions, respectively. These ERPs included both rotated and non-rotated
377 trials, but excluded the baseline trials. We also computed “veridical feedback” ERPs by selecting
378 the baseline trials preceding the onset of the feedback rotation. Each participant experienced
379 60 of such trials (15 per block), during which the visual feedback angle was always equal to the
380 reach angle, such that there was no experimentally imposed SPE.

381 We computed ERPs to test a correlation, across participants, between behavioral
382 learning rate and the average neural response to feedback during the adaptation portion of all

visuomotor rotation blocks. These ERPs included all trials in the visuomotor rotation condition except the baseline trials, and are deemed the “adaptation” condition.

Although we did not provide explicit reward feedback in the visuomotor rotation task, RPE could still occur as participants evaluate the accuracy of each movement. We designed the task to minimize RPE by making the target large enough so that almost all movements would result in endpoint feedback within the target. To test for an effect of RPE in the visuomotor rotation task, we sorted trials in the adaptation portion of the visuomotor rotation blocks by the absolute value of the angle of visual feedback relative to the center of the target. We created “most accurate” ERPs for each participant by selecting the 75 trials with the smallest absolute feedback angle, and “least accurate” ERPs by selecting the 75 trials with the largest absolute feedback angle.

**Feedback Related Negativity Analysis:**

The FRN was analyzed using a difference wave approach with ERPs recorded from FCz, where it is typically largest (Holroyd and Krigolson, 2007). Difference waves were computed for each participant by subtracting ERPs corresponding to unsuccessful outcomes from those corresponding to successful outcomes. To test for the statistically significant presence of the FRN for each difference wave, we submitted the mean value between 200-350 ms after feedback presentation to a one sample *t*-test against zero. This time window was chosen a priori on the basis of previous reports (Walsh and Anderson, 2012). To assess differences in FRN amplitude between experimental conditions and individual participants, we chose the peak

amplitude of the difference wave from 200-350 ms as a more sensitive measure of FRN amplitude (Holroyd et al., 2011). We used peak amplitude instead of mean amplitude because the time course of the FRN is not strictly described by our time window, although the peak should reliably occur within this window.

*Reward Learning Task:* The expected non-reward ERP was subtracted from the expected reward EPR to create an "expected" difference wave, and the unexpected non-reward ERP was subtracted from the unexpected reward EPR to create an "unexpected" difference wave.

We used a paired *t*-test to test the difference between peak FRN amplitude for the "expected" and "unexpected" difference waves. To compare the "expected" and "unexpected" difference waves, we estimated the "expected" difference wave using randomly selected trials from the "expected" conditions so that the number of trials averaged in the expected reward and expected non-reward ERPs would be matched to that in the unexpected reward (M=73.86 trials SD = 12.74) and unexpected non-reward ERPs (M=61.14 trials SD = 7.84), respectively, for each participant. This procedure was necessary because the maximum amplitude of ERPs are affected by signal-to-noise ratio and there were more trials in the expected condition than the unexpected condition.

*Visuomotor Rotation Task*: First, we created difference waves to test whether the rotations imposed on randomly selected trials elicited FRN. The “rotated 0.75 degrees” ERPs were subtracted from the “non-rotated 0.75 degrees” ERPs to create a “small VMR” difference wave.

The “rotated 1.5 degrees” ERPs were subtracted from the “non-rotated 1.5 degrees” ERPs to create a “large VMR” difference wave.

Next, we created a difference wave to test whether a FRN was observable by comparing trials where the endpoint feedback was furthest from the center of the target from those where feedback was closest to the center of the target. The “least accurate” ERPs were subtracted from the “most accurate” ERPs to create an “endpoint error” difference wave.

**P300 analysis:**

To analyze the P300 we used ERPs recorded from channel pZ, where it is typically largest (Fabiani et al., 1987). We calculated P300 amplitude as peak-to-peak voltage difference between the maximum peak occurring 250-500 ms after stimulus onset and the minimum preceding peak that occurred at least 100 ms after stimulus onset.

*Reward Learning Task:* We tested for differences in P300 amplitude between feedback conditions using 2 way repeated measures ANOVA with factors reward (levels: rewarded, non-rewarded) and expectancy (levels: unexpected, expected). P300 amplitude was calculated separately for the “unexpected reward”, “expected reward”, and “unexpected non-reward”, and “expected non-reward” feedback condition ERPs, described above. ERPs were estimated using a randomly selected subset of trials from each feedback condition to match the number of trials across cells on an individual participant basis (mean: 60.23 trials, SD: 8.5).

445 *Visuomotor Rotation task:* We tested for differences in P300 amplitude between trials with
446 rotated feedback and non-rotated feedback using two-way repeated measures ANOVA with
447 factors rotation (levels: non-rotated, rotated) and rotation magnitude (levels: 0.75 Degrees, 1.5
448 Degrees). P300 amplitude for each condition was calculated using the "rotated 0.75 degrees",
449 "non-rotated 0.75 degrees", "rotated 1.5 degrees" and "non-rotated 1.5 degrees", ERPs,
450 described above. ERPs were estimated using a randomly selected subset of trials from each
451 feedback condition to match the number of trials across cells on an individual participant basis
452 (mean: 77 trials, SD: 19.62).

453 We tested for differences in P300 amplitude between experimental conditions in the
454 visuomotor rotation task, irrespective of the randomly imposed rotations, using one-way
455 repeated measures ANOVA with three levels (veridical feedback, small error, and large error).
456 P300 amplitude for each condition was calculated using the "veridical feedback", "small error",
457 and "large error", feedback condition ERPs, described above. ERPs were estimated using a
458 randomly selected subset of trials from each feedback condition, to match the number of trials
459 across cells on an individual participant basis (mean: 53.84 trials, SD: 9.67).

460

461 **Results**

462 ***Behavioral Results***

463 *Reward Learning Task.* In the reward learning task participants adapted their reach angle on the
464 basis of binary reward feedback (Fig 3). We calculated a reward learning score for each subject
465 by subtracting the average reach angle in the clockwise learning condition from that in the

466 counterclockwise learning condition, excluding the baseline trials, such that the average reward
467 learning score would be approximately zero if participants did not respond to the reward
468 feedback in any way. We observed a mean reward learning score of 5.6 (SD = 5.6), which is
469 significantly greater than zero (one-sample *t* test; t(12) = 3.6, p = .004). Participants received
470 reward on 66.5% (SD = 5.9%) of trials in the high probability condition and 39.23% (SD = 4.9%)
471 of trials in the low probability condition.

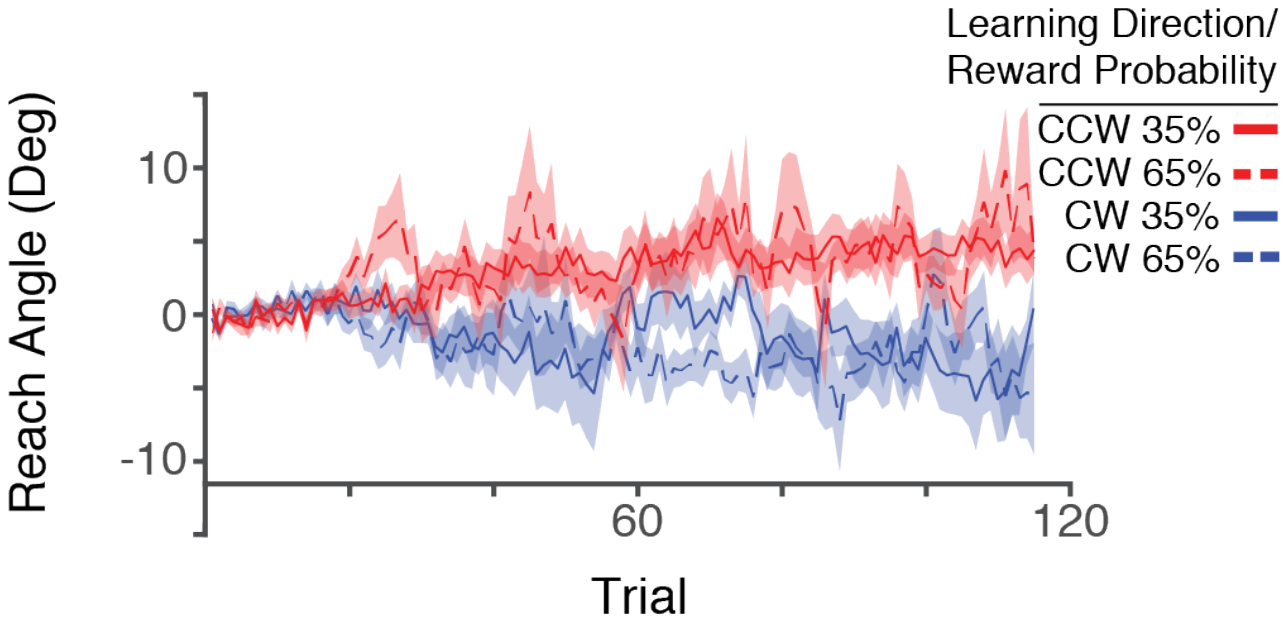


472

473 ***Figure 3***. *Participants adapted their reach angle in the reward learning condition. Group average reach angles in*
474 *the reward learning conditions are plotted. Each participant completed four blocks. For each direction of intended*
475 *learning (clockwise and counter clockwise), each participant completed a block in the high reward probability (35%)*
476 *condition and a block in the low reward probability (65%) condition. Shaded regions are +- 1 SEM.*

477

478 *Visuomotor rotation task*. In the visuomotor rotation task participants received endpoint cursor
479 feedback and adapted their reach angles in response to the rotated cursor feedback imposed

on randomly selected trials. To estimate trial-by-trial learning rates for individual participants we quantified the linear relationship between the change in reach angle after each trial with the rotation imposed on the preceding trial as the predictor variable. We took unsigned value of the resulting slope as a measure of learning rate, as it reflected the proportion of visuomotor rotation that each participant corrected with a trial-by-trial adaptive process. The mean learning rate was 0.4 (SD = 0.2), which was significantly different from zero (one-sample *t*-test; $t(12) = 7.85$, $p < .001$). This indicates that participants corrected for visual errors on a trial-by-trial basis. Figure 4 shows the average change in reach angle for each size and direction of the imposed cursor rotation.

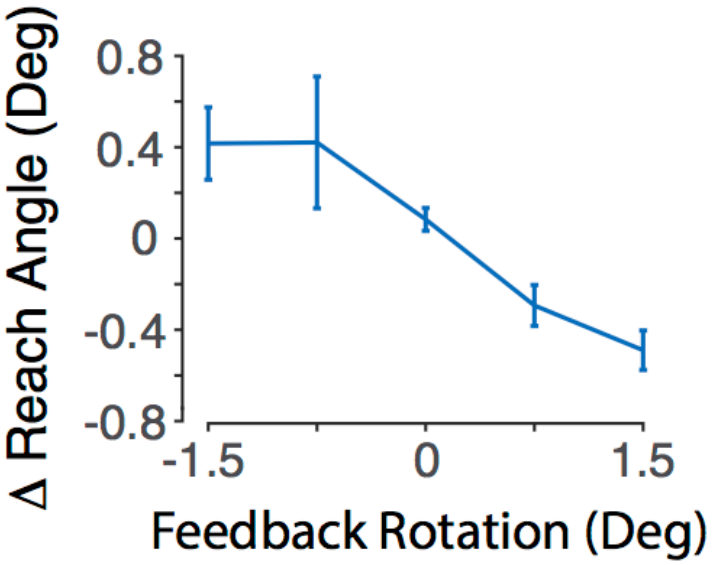


***Figure 4.*** *Participants adapted their reach angle on a trial-by-trial basis in the visuomotor rotation condition. For each size and direction of rotation, the average change in reach angle was opposite to the rotation, indicating that participants adapted their reaches to counteract the perturbations.*

**Feedback Related Negativity Results:**

*Reward Learning Task*

Figure 5a shows the ERPs recorded from electrode FCz during the reward learning condition, averaged across participants. The mean value of the "expected" difference wave recorded from FCz between 200-350 *ms* was significantly different from zero (M= 4.51 $\mu$v, SD=3.92, t(12)=4.14, p=.001, 1 sample *t*-test), indicating that expected feedback elicited a FRN in our reward learning task. The mean value of the "unexpected" difference wave was also significantly larger than zero (M= 5.77 $\mu$v, SD=2.74, t(12)=7.59, p<.001, one-sample *t* test), indicating that unexpected feedback also elicited a FRN.

The peak amplitude of the "unexpected" difference wave (M= 11.62 $\mu$v, SD=3.75) was larger than the peak amplitude of the "expected" difference wave (M= 8.92 $\mu$v, SD=3.77), (t(12) = -2.94, p = .012, paired *t* test; Fig 5b). This result indicates that FRN amplitude is modulated by probability of reward. This result is consistent with the theory that the FRN encodes RPE with respect to expected value that is proportional to the probability of reward.

"Expected" difference wave amplitude was significantly correlated to reward learning scores, which we calculated for each subject as the difference in average reach angle between the clockwise and counterclockwise learning conditions (r = .642, p = .018; Fig 5b). The "unexpected" difference wave amplitude was not correlated to reward learning scores (r= -0.048, p = .88; Fig 5b).

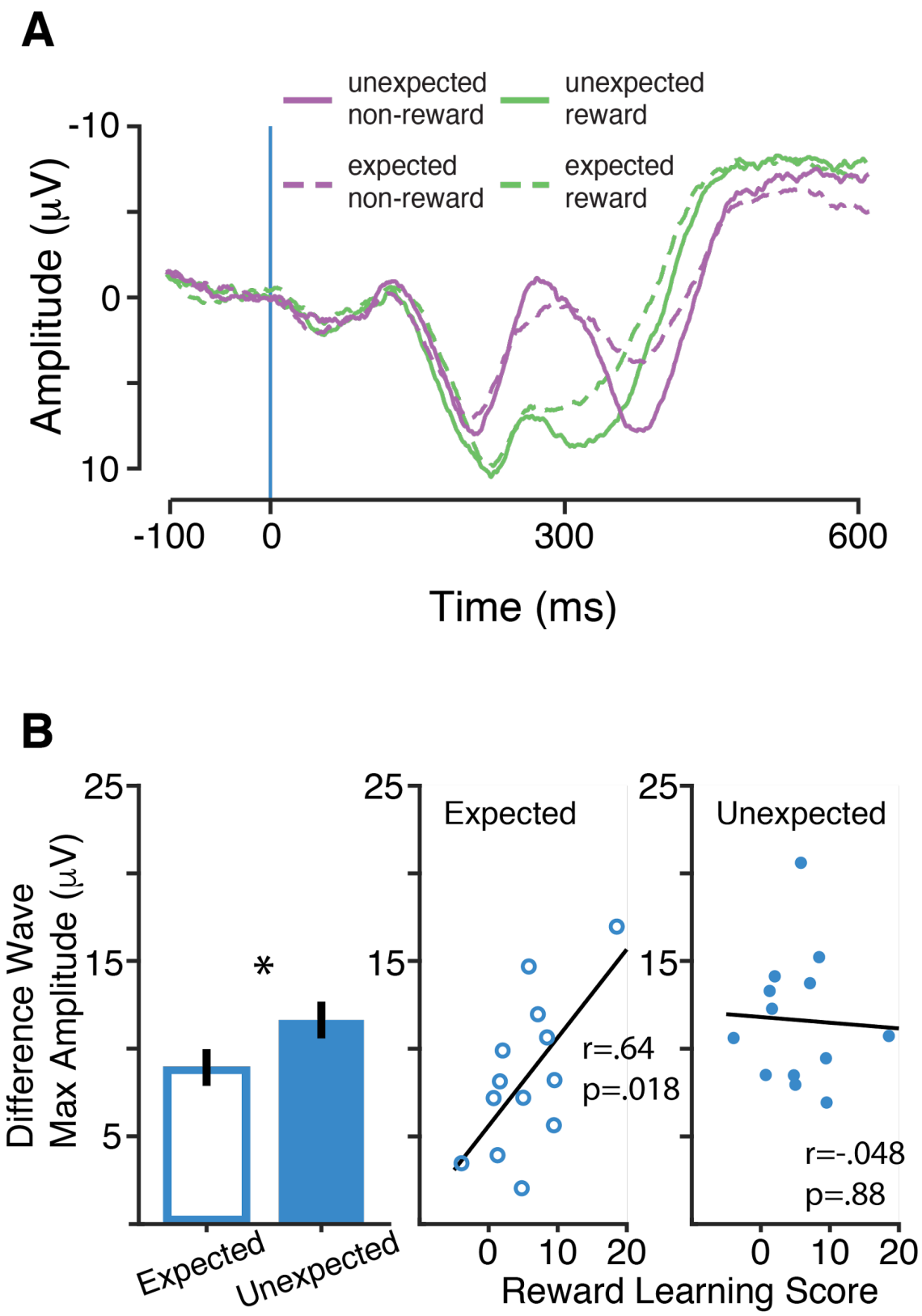
A
unexpected non-reward
unexpected reward
expected non-reward
expected reward
Amplitude (μV)
-10
0
10
-100
0
300
600
Time (ms)
B
Difference Wave Max Amplitude (μV)
25
15
5
*
Expected
Unexpected
Expected
r=.64
p=.018
Unexpected
r=-.048
p=.88
0
10
20
Reward Learning Score

512

***Figure 5.*** *The feedback related negativity reflects reward prediction error during the reward learning task.* ***A,*** *Trial averaged ERPs recorded from electrode FCz aligned to feedback presentation (0 ms: vertical blue line). Expected and unexpected reward reflects reward feedback in the high and low reward probability conditions, respectively. Expected and unexpected non-reward refers to non-reward feedback in the low and high reward probability conditions, respectively.* ***B,*** *The peak amplitude of the difference wave (reward ERP – non-reward ERP) between 200-350ms is larger for unexpected feedback than for expected feedback (Error bars: ±SEM). The peak amplitudes of the difference waves are correlated to behavioral learning scores across participants for the expected feedback, but not the unexpected feedback.*

*Visuomotor Rotation Task*

The mean value of the "small VMR" difference wave recorded from FCz between 200-350 ms was not significantly different from zero (M= -0.20 $\mu$v, SD=1.31, t(12)=-0.553, p=0.59, one-sample *t* test). Similarly, the mean value of the "large VMR" difference wave recorded from FCz between 200-350 ms was not significantly different than zero (M= -0.038 $\mu$v, SD=0.97, t(12)=-0.14, p=.89, one-sample *t* test). These findings indicate that the VMRs imposed in the visuomotor rotation task did not reliably elicit a FRN.

The mean value of the “endpoint error” difference wave recorded from FCz between 200-350 ms was not significantly different than zero (M= 1.18 $\mu$v, SD=3.23, t(12)=1.32, p=.21, one-sample *t* test), indicating that a FRN did not reliably occur on the basis of endpoint error feedback. The fact that we were able to detect a FRN in the reward learning task but not in the visuomotor rotation task is consistent with the notion that the FRN reflects RPE, and that our experimental design successfully dissociated RPE from SPE.

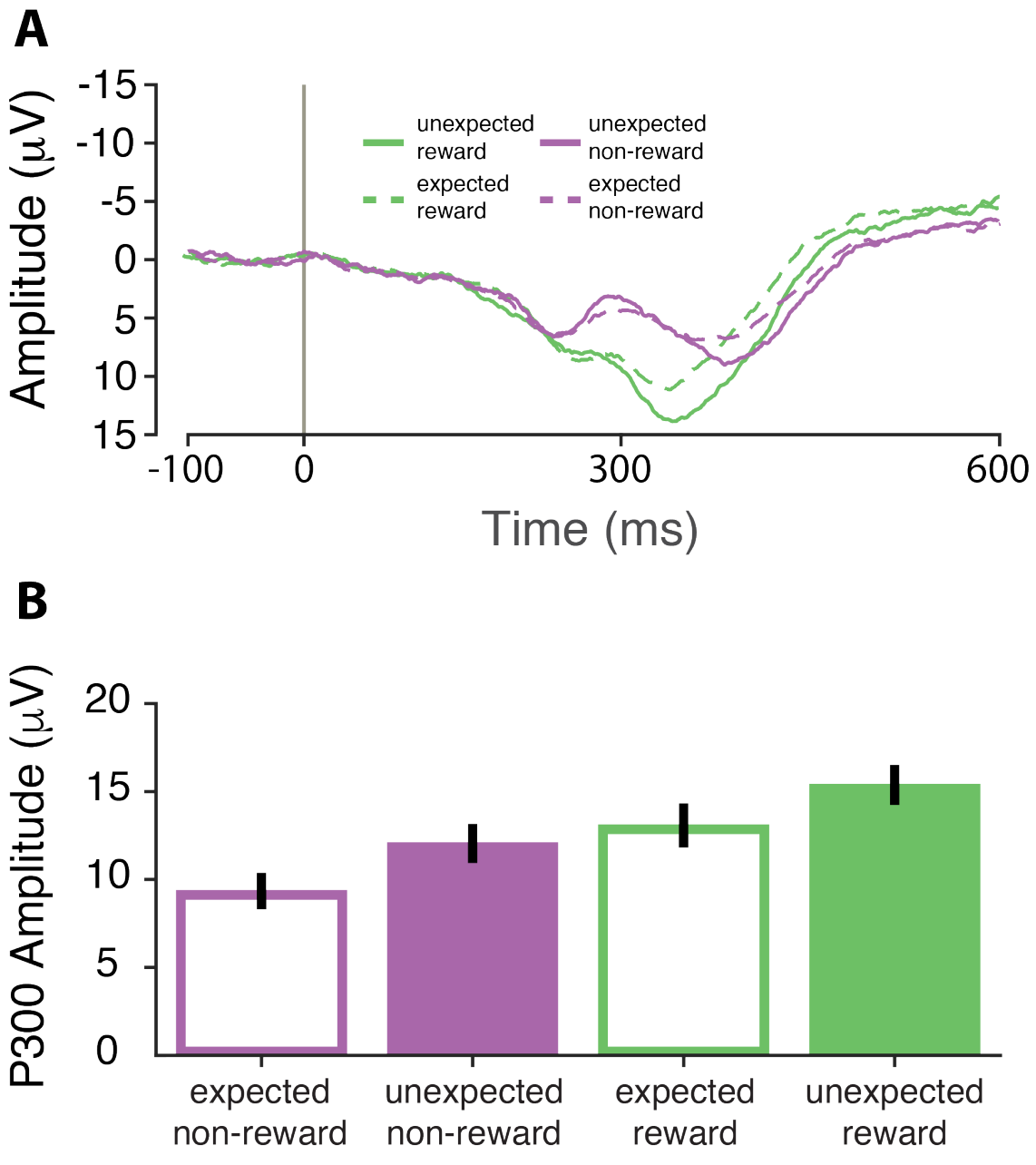


***Figure 6.*** *The P300 is modulated by feedback during the reward learning task.* ***A,*** *Trial averaged ERPs recorded from electrode Pz aligned to feedback presentation (0 ms: vertical line).* ***B,*** P300 amplitude in each feedback condition *(Error bars: +- SEM).* P300 amplitude is larger for rewarded feedback relative to unrewarded feedback, and unexpected feedback relative to expected feedback.

**P300 Results:**

*Reward Learning Task:*

Figure 6A shows ERPs recorded from electrode Pz during the reward learning condition, averaged across participants. We performed a 2x2 repeated measures ANOVA on P300 amplitude with factors expectancy and reward. Figure 6b shows P300 amplitude for each condition, averaged across participants  We found a significant main effect of feedback expectancy ($F(1,12) = 25.16$, $p<.001$), indicating that P300 amplitude was significantly larger in the unexpected feedback conditions. We also found a significant main effect of reward, ($F(1,12) = 23.81$, $p<.001$), indicating P300 amplitude was larger following rewarded trials compared to unrewarded trials. P300 amplitude was not significantly correlated to reward learning scores for any of the four feedback conditions:  expected reward ($r = 0.4$, $p = 0.17$) , unexpected reward ($r = 0.36$, $p = .22$), expected non-reward ($r = 0.14$, $p = .64$), and unexpected non-reward ($r = 0.28$, $p = .35$).

*Visuomotor Rotation Task*

Figure 7a shows ERPs recorded from electrode Pz during the visuomotor rotation task, averaged across participants. We first tested for an effect of the visuomotor rotation on P300 amplitude by comparing non-rotated feedback trials and rotated feedback trials. We performed a two-way repeated measures ANOVA with factors *presence of rotation* and *size of rotation*. We did not find significant main effects of *presence of rotation* ( $F(1,12) = 0.489$ , $p = .498$), *size of*

*rotation* (F(1,12)=1.564, p = .235), or an interaction between *presence of rotation* and rotation magnitude ( F(1,12) = 2.48 , p = .358).

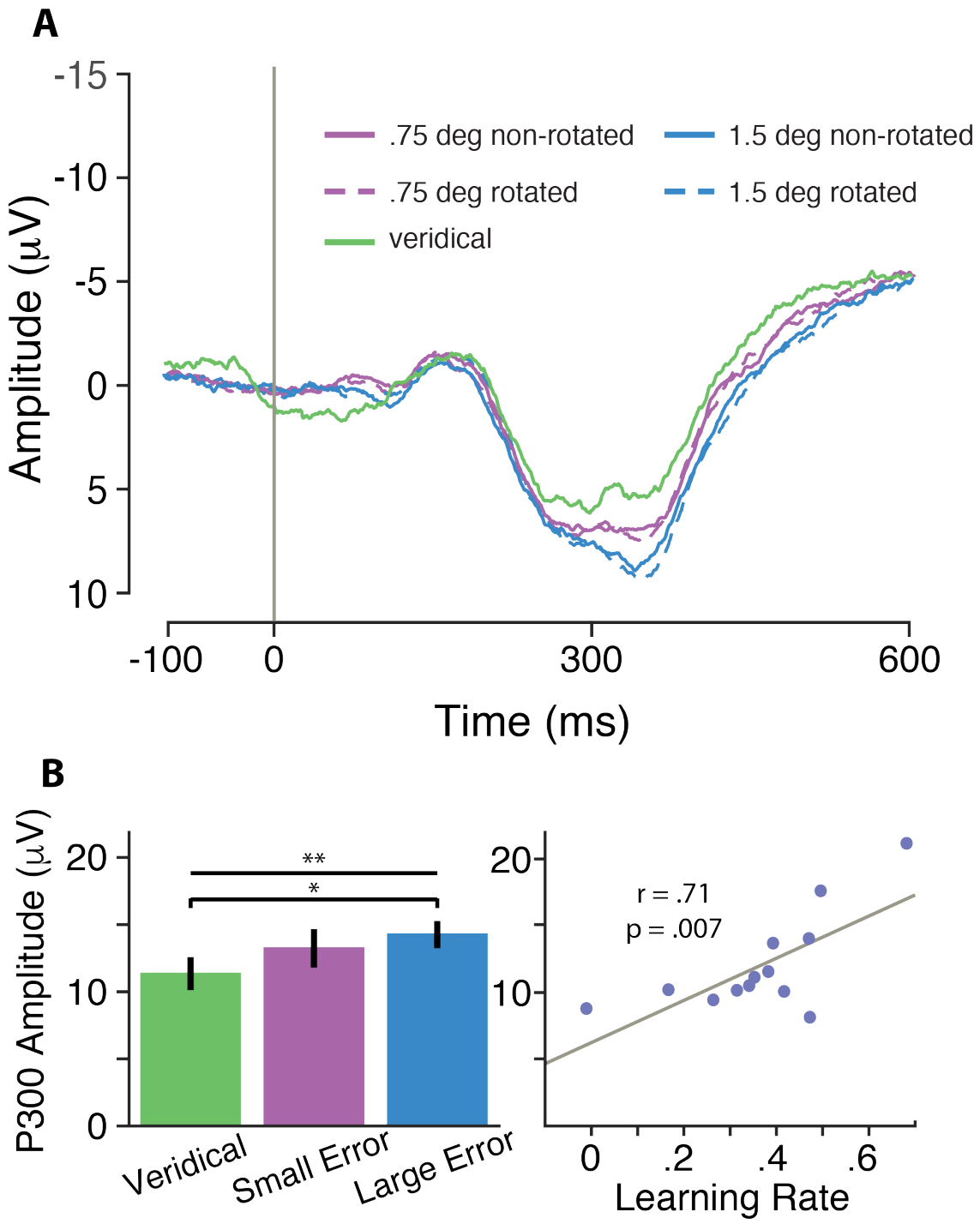

564 ***Figure 7.*** *The P300 reflects sensory error processing during the visuomotor rotation task.* ***A,*** *Trial average ERPs*
565 *recorded from electrode Pz aligned to feedback presentation (0 ms).* ***B,*** *The peak-to-peak amplitude of the P300*
566 *differs between the veridical feedback, small error, and large error conditions (Error bars: +- SEM). P300 amplitude*
567 *during adaptation was correlated to learning rate. *: p < .05, **: p < .01*

568

569 Next, we tested for an effect of experimental condition on P300 amplitude by
570 comparing baseline trials, small error trials, and large error trials. We found a significant main
571 effect of experimental condition ( $F(2,24) = 5.662$, $p = 0.01$; Fig 6b ). *Post-hoc* tests revealed
572 that the P300 amplitude was significantly greater in the "large error" condition than the
573 baseline condition ($t(12)=3.205$, $p = 0.023$, Bonferroni Corrected).

574 We also found a significant correlation between behavioral learning rate and the P300
575 amplitude measured in the "adaptation" condition ERPs ( $r = .708$, $p = 0.0067$; Fig 6b).

576

577 **Discussion**

578 We observed neural correlates of RPE and SPE during motor adaptation in reaching tasks
579 designed to isolate each response. Both tasks produced comparable changes in reach angle
580 through discrete feedback delivered at movement endpoint. By examining ERPs elicited by
581 feedback after each movement, we avoided potential confounds caused by neural activity or
582 artifacts related to movement execution, motion of the limb, and online error correction. We
583 observed that the feedback related negativity potential (FRN) encoded RPE in response to
584 binary reward feedback but the FRN was not elicited by sensory error feedback. The P300
585 occurred in response to both reward and sensory error feedback, and in each case P300

amplitude was modulated by feedback parameters such as expectancy, reward, and sensory error. In the visuomotor rotation task, the P300 was modulated by the size of SPE, and P300 magnitude was correlated to learning rate across participants. This suggests that the P300 might reflect a process that is involved in the processing of SPE for motor adaptation.

**The FRN Encoded Reward Prediction Error in Reward Based but not Sensory Error Based Motor Adaptation**

Although motor adaptation has traditionally focused on sensory error learning, recent work suggests that reinforcement learning processes can also contribute to motor adaptation (cite). In the present study, RPE was isolated from SPE during the reward learning task by providing only binary reward feedback in the absence of precise visual information concerning the position of the hand. This feedback elicited a well characterized fronto-central ERP component called the FRN.

In reinforcement learning theory, RPE is the difference between the observed outcome value and the expected value. The expected value of an action is equal to the product of reward magnitude and the estimated probability of reward. In our reward learning task the reward magnitude was binary (0 or 1), thus the expected value of a particular action on each trial (e.g. the direction of hand movement) was directly proportional to the probability of reward. Therefore, reward feedback should always elicit a positive RPE with increasing magnitude when reward is less probable. Conversely, non-reward should always elicit negative RPE with increasing magnitude when reward is more probable.

The FRN was observed in the reward learning task as a difference in voltage between ERPs elicited by non-reward feedback and those elicited by reward feedback. This difference was larger for improbable feedback than for probable feedback. This is consistent with a body of literature indicating that the FRN encodes a signed RPE (Holroyd and Krigolson, 2007; Holroyd et al., 2011; Walsh and Anderson, 2012). However, this result is not consistent with some recent reports suggesting that the FRN reflects an unsigned RPE value known as a surprise signal (Hauser et al., 2014).

A prominent theory proposes that the FRN reflects activity originating in the anterior cingulate cortex driven by phasic dopaminergic signaling of RPE (Holroyd and H, 2002; Santesso et al., 2009). This activity is purported to underlie reward-based learning processes by integrating RPE to affect future action selection. We sought to examine the role of the FRN in learning by testing the correlation between the amplitude of the FRN and the extent of learning as assessed behaviorally.

In typical reward learning paradigms, learning is associated with increased reward probability (cite), and as such the relationship between the FRN and the magnitude of learning is confounded by an effect of reward probability on FRN amplitude. In the current study, the reward learning task was adaptive to learning such that the overall reward probability was largely decoupled from the extent of adaptation. We found that the extent of behavioral learning was correlated to the peak amplitude of the FRN for the expected feedback condition but not the unexpected feedback condition. One possible explanation for this discrepancy is that participants responded reliably to the large RPEs as they were most salient, but the limiting factor in learning was a sensitivity to small RPEs. Even though small RPEs should produce less

629 learning per trial than large RPEs, in our task they were by definition more numerous and as
630 such could contribute comparably to the overall extent of learning. Another possibility is that
631 the measure of FRN amplitude became less reliable in the unexpected feedback condition due
632 to interference by surprise related signals that were not directly related to RL, such as the P300.
633 Relationships between the FRN and learning have been observed for tasks such as time
634 estimation and discrete motor sequence learning (Holroyd and Krigolson, 2007; van der Helden
635 et al., 2010). As such, the present findings support the idea that the same RPE processing
636 mechanism can drive learning across both cognitive and motor tasks.

637 In the present study, the sensory error-based learning task allowed us to dissociate the
638 neural signatures of RPE from those of SPE. SPE often coincides with RPE, as failure to achieve
639 the expected sensory consequences of a motor command usually entails failure to achieve the
640 subjective goal of the task. Our visuomotor rotation task was designed to elicit learning through
641 SPE while minimizing RPE, as the perturbations were relatively small and rarely resulted in
642 cursor feedback outside of the target. We did not observe the presence of the FRN in response
643 to sensory error feedback, despite clear adaptation.

644 Our results suggest that the ERP responses to RPE and SPE can be dissociated in motor
645 adaptation, and that the FRN is specific to reward based learning processes. Although the FRN
646 is classically associated with reinforcement learning, recent work has identified the FRN or the
647 closely related ERN in various motor learning and execution tasks involving sensory error
648 signals. These studies either concluded that reinforcement and sensory error based learning
649 processes share common neural resources, or they simply fail to distinguish between these two
650 processes altogether (Krigolson et al., 2008; Torrecillos et al., 2014; MacLean et al., 2015). We

651 argue that the brain processes RPE and SPE through distinct mechanisms, but that the two
652 processes can be confounded when perturbations causing a SPE are also evaluated as an
653 implicit failure to meet task goals. In this case, the brain could process a RPE and a SPE
654 independently, although learning might be driven primarily by the SPE. This is consistent with
655 behavioral studies showing that sensory error based learning is the primary driver of behavioral
656 change when both reward and sensory feedback is provided (Izawa and Shadmehr, 2011;
657 Cashaback et al., 2017).

658

659 **The P300 is Modulated by SPE and Surprise**

660 During the visuomotor rotation task in the present study, we observed a P300 ERP in response
661 to reach endpoint position feedback, and we found that P300 amplitude was modulated by the
662 size of SPE and was correlated to behavioral learning rate. Learning in visuomotor rotation
663 paradigms is thought to be driven primarily by SPE, and as such our findings suggest that the
664 P300 observed in this task might reflect neural activity that is specifically related to processing
665 of SPE underlying motor adaptation (Izawa and Shadmehr, 2011).

666 It is important to note that a P300 response is typically elicited by stimulus processing in
667 tasks unrelated to sensory error-based adaptation, including the reward learning task in the
668 present study. In our reward learning task, P300 amplitude was modulated by feedback valence
669 and expectancy but was not correlated to learning. A prominent and enduring theory proposes
670 that the P300 reflects cortical processing related to the updating of a neural model of stimulus
671 context upon processing of unexpected stimuli (Donchin, 1981; Donchin and Coles, 1988;

Polich, 2007). This theory resembles an account of sensory error adaptation in which the updating of an internal model of motor dynamics occurs when sensory input differs from the predictions of the internal model (Wolpert et al., 1995; Synofzik et al., 2008). It is possible that the P300 reflects an aspect of predictive processing that is common to both sensorimotor and cognitive function. The P300 is typically localized to parietal regions, which are implicated in processing SPE during adaptation to visuomotor rotation (Bledowski et al., 2004; Diedrichsen et al., 2005; Linden, 2005; Tanaka et al., 2009). Consistent with the P300 underlying SPE processing, cerebellar damage impairs sensory error based adaptation and causes P300 abnormalities (Tachibana et al., 1995; Martin et al., 1996; Maschke et al., 2004; Paulus et al., 2004; Smith and Shadmehr, 2005; Mannarelli et al., 2015).

Previous studies have examined P300 responses elicited by sensory error feedback. It has been demonstrated that P300 amplitude decreases along with the magnitude of reach errors during the course of prism adaptation (MacLean et al., 2015). This suggests that the P300 is modulated by SPE, but it does not rule out the possibility that the P300 simply attenuated with time. The P300 has also been reported to occur in response to another type of visuo-spatial error—random shifts in target location (Krigolson et al., 2008), although learning does not reliably occur in response to random target errors (Diedrichsen et al., 2005). Both of these studies also reported FRN components occurring in response to task errors. In the present study a P300 response was observed that is correlated to behavioral learning, and isolated from the FRN.

694 **References**

695 Bédard P, Sanes JN (2014) Brain representations for acquiring and recalling visual-motor
696 adaptations. Neuroimage 101:225–235.

697 Bledowski C, Prvulovic D, Hoechstetter K, Scherg M, Wibral M, Goebel R, Linden DEJ (2004)
698 Localizing P300 generators in visual target and distractor processing: a combined event-
699 related potential and functional magnetic resonance imaging study. J Neurosci 24:9353–
700 9360.

701 Cashaback JGA, McGregor HR, Mohatarem A, Gribble PL (2017) Dissociating error-based and
702 reinforcement-based loss functions during sensorimotor learning. PLoS Comput Biol
703 13:e1005623.

704 Delorme A, Makeig S (2004) EEGLAB: an open source toolbox for analysis of single-trial EEG
705 dynamics including independent component analysis. J Neurosci Methods 134:9–21.

706 Diedrichsen J, Hashambhoy Y, Rane T, Shadmehr R (2005) Neural Correlates of Reach Errors. J
707 Neurosci 25:9919–9931.

708 Donchin E (1981) Surprise!… Surprise? Psychophysiology 18:493–513.

709 Donchin E, Coles MGH (1988) Is the P300 component a manifestation of context updating?
710 Behav Brain Sci 11:357–374.

711 Fabiani M, Gratton G, Karis D, Donchin E, Others (1987) Definition, identification, and reliability
712 of measurement of the P300 component of the event-related brain potential. Advances in

713 psychophysiology 2:78.

714 Galea JM, Mallia E, Rothwell J, Diedrichsen J (2015) The dissociable effects of punishment and
715 reward on motor learning. Nat Neurosci 18:597–602.

716 Galea JM, Ruge D, Buijink A, Bestmann S, Rothwell JC (2013) Punishment-Induced Behavioral
717 and Neurophysiological Variability Reveals Dopamine-Dependent Selection of Kinematic
718 Movement Parameters. J Neurosci 33:3981–3988.

719 Glimcher PW (2011) Understanding dopamine and reinforcement learning: The dopamine
720 reward prediction error hypothesis. Proc Natl Acad Sci U S A 108:15647–15654.

721 Hauser TU, Iannaccone R, Stämpfli P, Drechsler R, Brandeis D, Walitza S, Brem S (2014) The
722 feedback-related negativity (FRN) revisited: New insights into the localization, meaning
723 and network organization. Neuroimage 84:159–168.

724 Holroyd CB, H G (2002) The neural basis of human error processing: Reinforcement learning,
725 dopamine, and the error-related negativity. Psychol Rev 109:679–709.

726 Holroyd CB, Krigolson OE (2007) Reward prediction error signals associated with a modified
727 time estimation task. Psychophysiology 44:913–917.

728 Holroyd CB, Krigolson OE, Lee S (2011) Reward positivity elicited by predictive cues.
729 Neuroreport 22:249–252.

730 Huang VS, Haith A, Mazzoni P, Krakauer JW (2011) Rethinking motor learning and savings in
731 adaptation paradigms: model-free memory for successful actions combines with internal

732 models. Neuron 70:787–801.

733 Inoue K, Kawashima R, Satoh K, Kinomura S, Sugiura M, Goto R, Ito M, Fukuda H (2000) A PET
734 study of visuomotor learning under optical rotation. Neuroimage 11:505–516.

735 Izawa J, Shadmehr R (2011) Learning from Sensory and Reward Prediction Errors during Motor
736 Adaptation. PLoS Comput Biol 7:e1002012.

737 Krakauer JW, Ghilardi M-F, Mentis M, Barnes A, Veytsman M, Eidelberg D, Ghez C (2004)
738 Differential Cortical and Subcortical Activations in Learning Rotations and Gains for
739 Reaching: A PET Study. J Neurophysiol 91:924–933.

740 Krigolson OE, Holroyd CB, Van Gyn G, Heath M (10/2008) Electroencephalographic correlates of
741 target and outcome errors. Exp Brain Res 190:401–411.

742 Linden DEJ (2005) The p300: where in the brain is it produced and what does it tell us?
743 Neuroscientist 11:563–576.

744 MacLean SJ, Hassall CD, Ishigami Y, Krigolson OE, Eskes GA (2015) Using brain potentials to
745 understand prism adaptation: the error-related negativity and the P300. Front Hum
746 Neurosci 9 Available at: http://www.ncbi.nlm.nih.gov/pmc/articles/PMC4464183/

747 Mannarelli D, Pauletti C, De Lucia MC, Currà A, Fattapposta F (2015) Insights from ERPs into
748 attention during recovery after cerebellar stroke: a case report. Neurocase 21:721–726.

749 Marko MK, Haith AM, Harran MD, Shadmehr R (2012) Sensitivity to prediction error in reach
750 adaptation. J Neurophysiol 108:1752–1763.

751 Martin TA, Keating JG, Goodkin HP, Bastian AJ, Thach WT (1996) Throwing while looking
752 through prisms. I. Focal olivocerebellar lesions impair adaptation. Brain 119 ( Pt 4):1183–
753 1198.

754 Maschke M, Gomez CM, Ebner TJ, Konczak J (2004) Hereditary cerebellar ataxia progressively
755 impairs force adaptation during goal-directed arm movements. J Neurophysiol 91:230–
756 238.

757 Mazzoni P, Krakauer JW (2006) An implicit plan overrides an explicit strategy during visuomotor
758 adaptation. J Neurosci 26:3642–3645.

759 Nikooyan AA, Ahmed AA (2015) Reward feedback accelerates motor learning. J Neurophysiol
760 113:633–646.

761 Paulus KS, Magnano I, Conti M, Galistu P, D'Onofrio M, Satta W, Aiello I (2004) Pure post–stroke
762 cerebellar cognitive affective syndrome: a case report. Neurol Sci 25:220–224.

763 Polich J (2007) Updating P300: an integrative theory of P3a and P3b. Clin Neurophysiol
764 118:2128–2148.

765 Santesso DL, Evins AE, Frank MJ, Schetter EC, Bogdan R, Pizzagalli DA (2009) Single dose of a
766 dopamine agonist impairs reinforcement learning in humans: Evidence from event-related
767 potentials and computational modeling of striatal-cortical function. Hum Brain Mapp
768 30:1963–1976.

769 Se P, J I, R S (2015) Reward-dependent modulation of movement variability., Reward-

770 Dependent Modulation of Movement Variability. J Neurosci 35, 35:4015, 4015–4024.

771 Shmuelof L, Huang VS, Haith AM, Delnicki RJ, Mazzoni P, Krakauer JW (2012) Overcoming Motor
772 "Forgetting" Through Reinforcement Of Learned Actions. J Neurosci 32:14617–14621a.

773 Smith MA, Shadmehr R (2005) Intact ability to learn internal models of arm dynamics in
774 Huntington's disease but not cerebellar degeneration. J Neurophysiol 93:2809–2821.

775 Synofzik M, Lindner A, Thier P (2008) The cerebellum updates predictions about the visual
776 consequences of one's behavior. Curr Biol 18:814–818.

777 Tachibana H, Aragane K, Sugita M (1995) Event-related potentials in patients with cerebellar
778 degeneration: electrophysiological evidence for cognitive impairment. Brain Res Cogn
779 Brain Res 2:173–180.

780 Tanaka H, Sejnowski TJ, Krakauer JW (2009) Adaptation to Visuomotor Rotation Through
781 Interaction Between Posterior Parietal and Motor Cortical Areas. J Neurophysiol
782 102:2921–2932.

783 Torrecillos F, Albouy P, Brochier T, Malfait N (2014) Does the processing of sensory and reward-
784 prediction errors involve common neural resources? Evidence from a frontocentral
785 negative potential modulated by movement execution errors. J Neurosci 34:4845–4856.

786 van der Helden J, Boksem MAS, Blom JHG (2010) The importance of failure: feedback-related
787 negativity predicts motor learning efficiency. Cereb Cortex 20:1596–1603.

788 Walsh MM, Anderson JR (2012) Learning from experience: event-related potential correlates of

789 reward processing, neural adaptation, and behavioral choice. Neurosci Biobehav Rev
790 36:1870–1884.

791 Wolpert DM, Ghahramani Z, Jordan MI (1995) An internal model for sensorimotor integration.
792 Science 269:1880–1882.